Electron-impact ionization of C^{3+} and N^{4+}

D. H. Crandall and R. A. Phaneuf

Oak Ridge National Laboratory, Oak Ridge, Tennessee 37830

P. O. Taylor*

Joint Institute for Laboratory Astrophysics, University of Colorado and National Bureau of Standards, Boulder, Colorado 80309

(Received 24 April 1978)

Measured cross sections for electron-impact ionization of C^{3+} and N^{4+} are reported for collision energies between threshold and 500 eV. The measurements were performed with crossed electron and ion beams. The peak cross sections obtained are 2.3×10^{-18} cm^2 near 200 eV for C^{3+} and 1.5×10^{-18} cm^2 near 400 eV for N^{4+} with good-confidence absolute uncertainties of $\pm 11\%$ and $\pm 15\%$, respectively. Comparisons of present data with the available theoretical estimates range from good agreement to discrepancies of a factor of two. At the highest energies of the present measurements, near 500 eV, the cross sections have not yet begun to decrease as predicted by all the available theories. It is postulated that inner-shell-electron excitation followed by autoionization is contributing to the measured ionization cross sections at these energies. Ionization-rate coefficients are derived from the data and compared with those measured in plasmas. The agreement in ionization rates is satisfactory in the C^{3+} case, but discrepancies of nearly a factor of two exist for the N^{4+} case.

I. INTRODUCTION

Ionization of atomic particles by electron impact is a fundamental process of intrinsic interest. The process is difficult to calculate reliably due to the presence of three independent particles in the final state. The earliest classical model of Thomson[1] derives a cross section by including all those collisions between two free electrons which result in energy transfer greater than the binding energy of the atomic electron. The result is then summed over the number of electrons on the atom at each binding energy. The cross sections obtained are remarkably close to reality[2,3]:

$$\sigma = c \sum_j \frac{r_j}{EI_j}\left(1 - \frac{I_j}{E}\right) \qquad (1)$$

(where c is a constant whose value depends on the units employed, r_j is number of electrons with binding energy I_j, and E is the collision energy). Many of the improved estimates have simply modified that part of Eq. (1) which is in parentheses and thus scaled the classical result to give better agreement with typical experimental values. In a review of electron-impact excitation and ionization, Bely and Van Regemorter[2] emphasize the difficulty of obtaining correct ionization theory and point out that developed methods are not rigorously satisfying, but that the various approaches generally give results in agreement with experiment to within a factor of 2 or better.

Exact quantum representation of the ionization process has not been formulated due to the difficulties of consistently representing the initial and final states of the system and the fields in which the two electrons move. However, Born and Coulomb-Born approximations have been developed[4,5] which in general obtain the correct behavior at asymptotically high collision energies, namely, that the cross sections decrease as $\log E/E$, in contrast to the classical behavior of Eq. (1). Coulomb-Born calculations for C^+, C^{2+}, O^+, O^{2+}, N^+, and N^{2+} (Ref. 6) and for a few other ions such as Mg^+ (Ref. 7) give agreement to about $\pm 25\%$ with crossed-beams experiments.[8-10]

Thus, in general, ionization cross sections can be estimated to within a factor of 2, and for neutral and singly or doubly charged ions there are specific experimental data and theoretical quantum approximations which give more reliable values. However, for the large number of partially stripped ions, available theory must be tested experimentally before accepted as accurate to better than a factor of 2, and little experimental data exist[3]; the present studies have been undertaken to fill this need. Two recent Coulomb-Born estimates of the ionization cross section for C^{3+} and N^{4+} are the calculation of Moores[11] (without exchange) and the scaled Coulomb-Born estimate for Li-like ions by Golden and Sampson[12] (based on cross sections calculated in Coulomb-Born with exchange for ions of infinite nuclear charge[13]). These two calculations agree well and compare favorably with present data, except at the highest experimental energies, where the measurements do not decrease as predicted. Recent calculations reported by Hahn,[14] using a modified Bethe approximation, fall below present data at the lower energies.

The most common physical situation in which

electron-impact ionization of multicharged ions is important occurs in high-temperature plasmas. Such plasmas occur naturally in astrophysical situations, and most of the efforts to provide ionization cross sections for multicharged ions have originated from astrophysical studies.[2,15] Laboratory studies of high-temperature plasmas have grown tremendously in recent years, especially in the effort to develop fusion energy reactors. Improvement in observational techniques and modeling of both astrophysical and laboratory plasmas has intensified the need for more reliable data on basic processes such as electron-impact ionization. As an example, more than half of the energy put into many present tokamak plasmas is returned as line radiation of impurity ions, which constitute only a small fraction of the plasma density.[16] Models of this radiation by impurity ions[17-19] have relied on the coronal equilibrium model from astrophysics,[20] but the models are being improved to more realistically represent the confined laboratory plasma. However, the models can never be more accurate than the basic input data which determine the state of ionization of impurity ions. These have relied on classical estimates of collisional ionization cross sections. There are plasma-observed ionization-rate measurements for the C^{3+} and N^{4+} ions,[21-23] which can be compared with present data to help evaluate accuracy of the techniques used in plasma observation.

II. TECHNIQUE

A. General method

The present experiments were performed with crossed beams of electrons and ions. The crossed-, charged-beams method of studying atomic collisions requires substantial technical sophistication but allows control and accurate measurement of most experimental parameters; the ability to systematically vary parameters permits detection and evaluation of spurious effects so that reliable results can be obtained. The colliding beams approach and most of the successful experiments have been reviewed recently by Dolder and Peart.[24]

For beams crossed at right angles, the relationship between measurable parameters and cross section for ionization of the ion beam by the electron is[24-26]

$$\sigma = \frac{R_{+1}}{I_q I_e} q e^2 \frac{v_q v_e}{(v_q^2 + v_e^2)^{1/2}} \frac{F}{E_{+1}}, \qquad (2)$$

where R_{+1} is the number of ions of charge $q+1$ created per unit time by the interaction of the beams of $N_q = I_q/qe$ incident ions per unit time and

$N_e = I_e/e$ incident electrons per unit time, and where v_q and v_e are the ion and electron velocities. The form factor F expresses the overlap of the spatial distribution of the two beams in the direction z, perpendicular to their interaction plane, and is given by[25]

$$F = \frac{\int i_q(z)\, dz \int i_e(z)\, dz}{\int i_q(z) i_e(z)\, dz}, \qquad (3)$$

which has units of length. The efficiency E_{+1} is the probability that an ion of charge $q+1$, created by interaction of the beams, will be detected. Measurement of the parameters in Eq. (2) allows direct determination of cross section for electron-impact ionization of the incident ion at collision velocity $v = (v_q^2 + v_e^2)^{1/2}$. Equation (3) assumes that F is independent of the beam-current distributions in their plane of intersection, since the beams completely overlap in this plane. This assumption requires that the transverse extent of the vertical scanning slit be wider than either beam, that their vertical distributions be measured at their point of intersection, and that the beams be sufficiently collimated that one does not diverge significantly within the transverse extent of the other—all of which are guaranteed in the present experiment.

B. Specific experimental arrangement

1. Overview

The experiment is shown schematically in Fig. 1. The geometry was chosen to minimize the background in the measured ionization rate arising from collisions of incident ions with residual gas; only the 15-cm path length between the purifier and the analyzer, which is at 1×10^{-9}-Torr pressure, can contribute to this background. Ions produced in the source were extracted at the acceleration voltage and analyzed to provide a beam with a specific charge-to-mass ratio (q/m). By the time the beam entered the high-vacuum chamber, a small fraction of the ions had changed charge through interaction with residual gas along the beam transport path. These unwanted charge states were removed by the charge purifier, an electrostatic parallel-plate analyzer operated with low resolution sufficient to isolate the original charge q at the original velocity v_q. The purified ion beam was crossed at 90° by a monoenergetic electron beam, and the ions then passed into the analyzer, which separated them according to final charge. The post-collision parallel-plate analyzer directed ions of charge $q+1$ to an additional 32° cylindrical analyzer and, finally, through cylinder lens focusing to a channel electron multi-
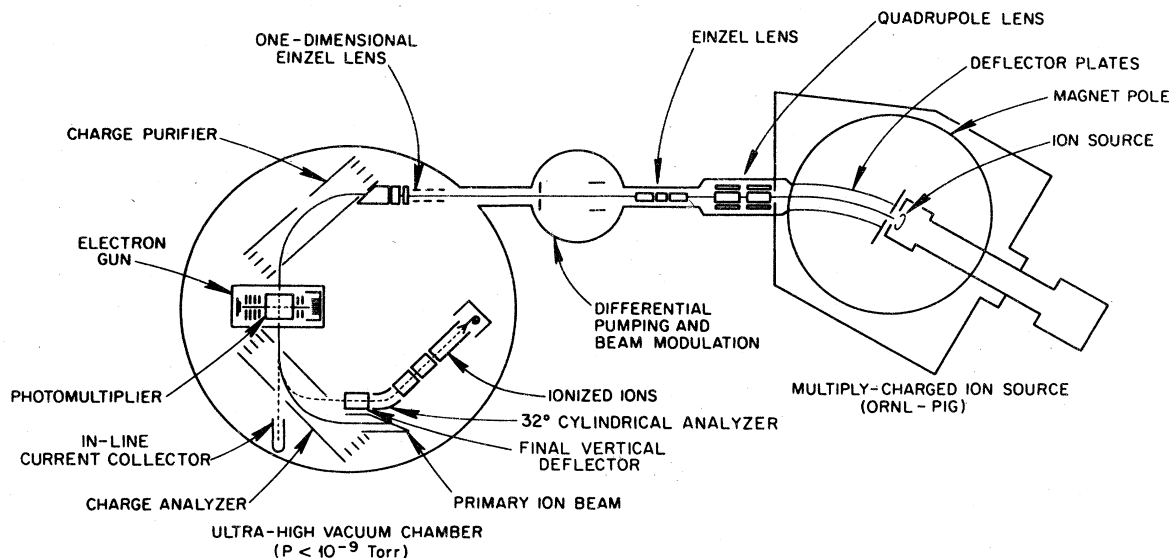
FIG. 1. Schematic overview of the complete experimental apparatus.

plier, where they were counted. When the parallel-plate analyzer was set to pass ions of charge $q+1$ to the channeltron, the incident beam of charge q was directed into a Faraday cup collector of sufficient spatial extent to collect ions of original charge q, for $q = 3+$, $4+$, or $5+$. The photomultiplier shown in Fig. 1 was used for experiments on electron-impact excitation, which are reported elsewhere.[27,28]

2. Ion source and transport

The ion source has been described previously.[29] It is a cold cathode, Penning ion gauge (PIG) source with ion extraction (acceleration) transverse to the magnetic field. Since the source is immersed in a magnetic field, the extracted ions begin cyclotron orbits, but extraction is into a region between the cylindrically curved plates that are used to apply an electrostatic field transverse to the magnetic field. By variation of the potential on these plates, a given charge-to-mass (q/m) ion species can be selected to pass through the exit aperture just outside the region where the two fields terminate. For the present experiments an acceleration potential of 10 kV was applied.

Transport of the ions from the source to the experiment was aided by both an electrostatic quadrupole lens and an einzel cylinder lens, with vertical and horizontal deflection also available. The gas load at the source was pumped by several 10-in. oil diffusion pumps, and the pressure in the region of the crossed electric and magnetic

field analyzer was about 1×10^{-6} Torr. The differential pumping section of the beam transport system was isolated from both the ion source and experiment vacuum chamber by combined apertures and tubes that restricted the gas flow; during experiments this section was maintained at pressures in the 10^{-8}-Torr range by a 4-in. oil diffusion pump with a refrigerated cold baffle. A beam-defining aperture (0.64 cm high and 0.32 cm wide) and deflection plates before the aperture combined to allow complete cutoff of the ion beam in the differential pumping section by application of about 100 V to the deflection plates.

3. Details of collision geometry

The collision chamber, 60-cm diam. and 30 cm deep (Fig. 1), contained the high-vacuum apparatus. The focusing properties of the parallel-plate analyzers[30] made it desirable to have additional independent ion-beam focusing in the vertical and horizontal planes. This was accomplished by two flat-plate, one-dimensional einzel lenses at the entrance to the chamber. In the vertical plane the beam was not strongly focused and remained nearly parallel throughout the chamber. The several apertures were all large $(H > 1.25$ cm) compared to the height of the beam, which was stopped down to less than 0.63 cm at the differential pumping and beam modulation section and measured to be typically 0.4-cm full height at the beam intersection (Fig. 2). Vertical deflectors— located at the second one-dimensional einzel lens, just before and just after the electron beam, and
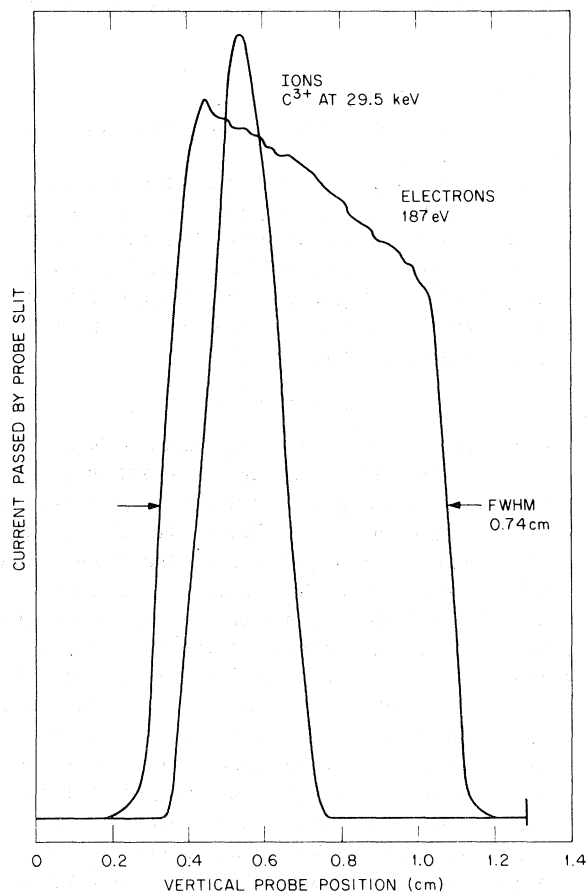
FIG. 2. Vertical distribution of beam currents at the collision center.

was chosen to accept a beam diverging from the parallel-plate analyzer exit and to focus that beam at infinity. Thus a nearly parallel beam of ions entered the final cylinder lens to be focused onto the channeltron. This three-element lens was operated as a strong focusing device with first element at ground, the second element at positive voltage, and the third element at negative voltage near the bias potential applied to the front of the channeltron, which was immersed within the third lens element.

The ion-beam size and divergence were restricted by the apertures at the purifier entrance and between purifier and collision center (4.5 cm from collision center) so that after the collision no ions would be lost before reaching detectors. For the several beam apertures, the location, horizontal dimension, and ion current lost to that aperture during typical data collection are given in Table I, where measurable.

The electron gun was only slightly modified from a version used in several previous crossed-beams experiments, and its characteristics are well documented.[31] The entire beam is immersed in a uniform permanent magnetic field which confines the electrons and allows maintenance of a high beam density. The electrons were accelerated from a hot cathode by a series of slotted plates which maintain a uniform electric field parallel to the magnetic field and thus minimize spiraling. The electrons were turned off by application of a negative voltage to one of the electrodes. Accurate electron energy values were established by onset of electron-impact excitation of $1s^2\,2p(^2P)$ level of C^{3+}.[27,28] The intersection of the beams occurred inside a stainless-steel box (roughly 4 cm long, 4 cm wide, and 2.5 cm high) with slots for beam passage and for passage of a vertical-scanning probe slit. The box was coated inside with gold black[32] to reduce light reflection and secondary particle scattering. The probe slit has a height of 0.02 cm and a width greater than either beam. The probe travels vertically through the collision chamber and can be rotated to intercept either beam. Figure 2 shows typical beam currents transmitted through this probe as a function of vertical slit position. The electron beam height is about 0.7 cm and its width is less than 0.2 cm. If the electrons were uniformly distributed vertically and the ion beam were contained entirely within the electron beam, then the form factor F of Eq. (2) would be equal to the electron beam height. Numerical evaluation of F for the data of Fig. 2 gives $F = 0.690$ cm.

A special collector for the electron beam was devised to minimize reflected electrons which would travel back through the collision box because

between the parallel-plate analyzer and 32° cylindrical analyzer—positioned the ion beam in the vertical direction.

The vertical position of the beam was complicated by the permanent magnetic field that confined the electrons. The 200-G field was perpendicular to the ion beam, extending a few centimeters to each side of the collision center. This field deflected the ion beam upward several degrees and was compensated by downward electrostatic deflection (800 V/cm) immediately before and after the collision center. Ions which changed their charge at the center of the electron-confining magnetic field could emerge with slightly different vertical trajectories than those passing through without a change in charge. Thus additional vertical deflection of the ionized beam at the exit of the parallel-plate analyzer was used to transmit these ions to the channeltron.

In the horizontal plane a parallel-plate analyzer provides focusing of the entrance aperture onto the exit aperture. The 32° cylindrical analyzer

TABLE I. Widths and currents to horizontal apertures in collision chamber.

	Width (cm)	Current[a]
2 cm before purifier	0.5	
Purifier entrance	0.24	0.1
Purifier exit	0.71	
4.5 cm before collision center	0.32	0.2
2.1 cm before collision center	0.5	
1.9 cm after collision center	0.63	$<10^{-5}$
4.4 cm after collision center	0.63	$<10^{-2}$
Analyzer entrance	1.0	10^{-5}
Analyzer exit (ionized ions)	1.2	

[a] Currents are fraction lost to that aperture relative to final cup-collected current. Apertures without currents listed were internally grounded.

of confinement along magnetic field lines. Secondary electrons can be held at the collector by bias potentials, but reflected primaries cannot. The electron collector was constructed of thin razor blades stacked with their sharp edges toward the beam so that an array of vertical knife edges spaced every 0.06 cm with a total surface of 1.3 $\times 1.3$ cm^2 and a 1.0-cm depth was located 6 cm after the beams intersection. The measured current to the collector for incident 100-eV electrons was 3% higher with collector biased between +50 and +350 V than with no bias, indicating that the fraction of secondary electrons escaping the unbiased collector was 3% of the primary current. Measurement of the current to electrodes that were on the entrance side of the collision region but shielded from primary electrons provided a rough estimate that 1% of the incident primary electrons were reflected, which is consistent with the expectation that the reflected primary fraction would be less than the number of escaping secondary electrons.[26]

To separate signal from background, a small on-line computer was used to switch beams and to switch on and off the scalers counting ionization events. Two scalers were gated so that one collected signal plus background counts with both beams on and the other collected counts from all background processes. The gating of the scalers included delays which allowed beam currents to stabilize after changes of switching voltages. Data were acquired with two different switching schemes, one which switched both beams and the other which left the ion beam on continuously and chopped only the electron beam. Since there was no detectable background when the electron beam alone was on, there was no difference in results from the two switching schemes, and the "elec-

trons only" switching was employed for most of the data.

C. Difficulties and uncertainties in detecting ionized ions

There are many sources of potential problems or error in the experiment, but the flexibility is available to test and quantitatively evaluate these problems. Since this is the first detailed report of work with this apparatus, the primary difficulties and associated uncertainties encountered are described here in some detail.

1. Counting sensitivity

Care must be exercised with channeltrons to assure that the entire opening (cone-shaped, 1-cm diam. in this case) is active in supplying secondary electrons which are multiplied in the body of the device. The potential just outside the channeltron opening must be near the potential at the surface of the device. Significant distortion of the electrostatic field near the surface of the cone-shaped entrance can either pull the first-created secondary electrons out of the channeltron or drive them so effectively down the surface that they do not attain multiplication trajectories. For channeltrons operated with front bias potential of about -3 kV, with nearby grounded surfaces and no field-straightening grids, it has been reported that the effective surface area sensitive to incident ions is reduced to about $\frac{1}{4}$ of the physical opening of the detector.[33] The efficiency of detecting an incident ion is reasonably asserted to be near 100% for ions in the energy range from a few keV[34] up to several tens of MeV,[35] provided care is taken with the field distribution near the entrance. In the present case, placing negative bias (about -3 kV) on the front of the channeltron accelerates the incident ions by their charge times the bias voltage and additionally repels stray secondary electrons incident from outside the device. To avoid grid structures in the ionized beam, the channeltron was immersed in the third element of the cylinder lens at the end of the 7 cm long by 2.5-cm diam. cylinder, and this element was operated slightly more negative than the front channeltron bias. In this way the potential near the channeltron surface was not appreciably disturbed by external fields, and the lens element both enhanced ion focusing and guarded the channeltron from external secondary electrons. A source of noise was presumably uv photons produced in the Faraday cup at the analyzer exit by the primary ion beam and was unaffected by voltages on either the 32° analyzer or the center element of the einzel lens. The-fact that the chan-

neltron response to this noise was observed to be constant for voltages on the third lens element within ± 200 V of the -3 kV detector front bias voltage was taken as evidence that the full channeltron opening was sensitive under such conditions. For diagnostic purposes the voltage of the third element was varied from normal operation with the following observations: (i) the background counting rate (presumably due to incident photons) reduced suddenly by about a factor of 3 when the third element was about -4 kV or more negative, implying that the sensitive area of the channeltron was reduced significantly from its 1-cm cone diam; and (ii) the apparent ionization cross section for $e^- + C^{3+} \rightarrow C^{4+}$ at 187 eV was reduced by 44% with the third element at -4 kV, implying that 44% of the ions created by beams interaction strike the channeltron outside this reduced sensitive area. Since the reduction in the counting of background photons was much greater than the reduction in apparent ionized ion signal, the size of the scattered ion beam was determined to be smaller than the full detector size as expected. Except for this diagnostic data, measurements were made with the third element of the einzel lens about 150 V more negative than the front of the channeltron.

2. Transmission of ions to the detector

Spatial size of incident ion-beam components relative to detectors is only part of the question of transmission of ion-beam components from the collision center to their detectors. Measurement of transmission of the primary beam to its Faraday cup collector was reasonably straightforward. As indicated in Table I, the current loss to apertures after the collision was found to be substantially less than 1%. With no voltage on the parallel-plate analyzer, the beam is transmitted through to the in-line Faraday cup behind the analyzer, as shown schematically in Fig. 1. The current to this collector was frequently compared with the current to the Faraday cup at the analyzer exit that collected the primary beam during acquisition of ionization data. The currents to the two collectors were never measurably different by a visual electrometer reading, and transmission of the primary ion beam is taken to be 99% or greater. The Faraday cup at the analyzer exit was preceded by a guard ring between the Faraday cup and back plate of the analyzer. The guard ring was operated at about -150 V to reject incident secondary electrons and retain any secondaries produced in the cup. This guarded Faraday cup was always compared to the in-line collector with the latter biased by about $+300$ V to retain

secondaries.

Only a few parts in 10^{10} of the incident ions are ionized to the next higher charge state by electron collisions, and measurement of transmission of these product ions from the collision center to the channeltron is more difficult. Any loss prior to the analyzers might reasonably be identical for the product ions and primary beam; it was found to be less than 1% for primary ions. To determine the transmission of ions through the two analyzers and cylinder lens, a number of slightly different measurements were performed. All of the measurements used the channeltron as an ion-current collector. The channeltron and electrometer to measure the collected ion current were floated at the normal channeltron bias voltage (-3 kV), and the third element of the cylinder lens was operated slightly more negative. Thus the secondary electrons from outside were repelled, but secondary electrons created by ions incident on the channeltron were held at the channeltron. This was the same arrangement as used for the collection of ionization data except that the whole channeltron was floated at bias potential, rather than the front at potential and the output end at ground. By changing the parallel-plate analyzer voltage, the incident ions were directed alternately to the channeltron or to the Faraday cup at the analyzer exit. Ion beams of the same species, charge, and velocity as the product ions from the electron-impact experiment were obtained for this transmission measurement in several different ways, including the extraction of ions directly from the ion source; the formation of ions by ionization in the drift tube, which could be selected by the purifier to pass through the interaction volume; and ionization along the 15-cm path between purifier and analyzer produced by adding N_2 gas to the collision chamber. To avoid damage to the channeltron, the various ion beams used for transmission measurements were never allowed to exceed 5×10^{-9} A. The average of seven separate measurements with different sources of ions and different ion-beam tuning is 0.918 ± 0.004 standard deviation (s.d.) for the ratio of channeltron current to analyzer Faraday cup current. The small statistical variation indicates that the measurement was quite independent of the source of ions and of changes in tuning-focusing parameters, which were varied over a wider range in transmission studies than in ionization data acquisition. It is not clear whether the failure to achieve the expected 100% transmission is really a failure to transmit all ions through the ion optics or a systematic problem in using the channeltron as a current collector. Thus, an absolute uncertainty of $\pm 8\%$ is assigned to the transmission, but the

value 0.918 is used to correct the data.

As mentioned, the ions additionally ionized by electrons in the center of the electron-confining magnetic field could have a slightly different vertical trajectory at the parallel-plate analyzer exit than would those ions which pass through all post-collision optics with their original charge. Thus the value of voltage used at the final vertical deflector to transport the test ion beam to the channeltron might not be quite correct for the transport of electron-impact ionized ions. Figure 3 shows that the electron-collision-produced ions were centered on the channeltron with zero vertical deflection by the final vertical deflector. However, test beams produced prior to the collision center (and its magnetic field) were centered on the channeltron by a 100-V downward deflection. Beam-deflection tests as shown on Fig. 3 were performed routinely to assure proper tuning of ions onto detectors.

3. Background

The most annoying difficulty in the experiment was background. The maximum real signal obtained was about 800 (c/sec)/μA of ions for C^{3+} ionized by 200-eV electrons. The ionization of incident ions by residual gas contributed a back-

ground which was quite small in the present experiment. By adding N_2 gas to the collision chamber to enhance this background, it was shown that for the present geometry at 1×10^{-9} Torr (typical operating pressure) fewer than 100 (c/sec)/μA of ions would occur for C^{3+} ions. Nevertheless, a background of about 5000 (c/sec)/ μA of ions was encountered for typical well-tuned ion beams. The background was somewhat dependent on focusing and deflecting parameters, but was almost independent of voltages applied to the 32° analyzer or to the center element of the cylinder lens. It was therefore concluded that background arose from photons produced by the incident ion beam. The photons are created principally within the primary ion-beam collector, and this background was reduced but not eliminated by coating with gold black those surfaces capable of reflecting photons towards the channeltron.

A small portion of this photon background was modulated by the space charge of the electron beam, giving rise to a small spurious signal. The typical change in the background caused by turning on the electron beam was about 5-(c/sec)/ μA ions for C^{3+} ions crossed by the 50-eV electron beam. Such cross modulation of the background produced by one beam by the space charge potential of the other beam is not new in this type of experiment[25] and can be analyzed by systematic variation of beam parameters. The effect was observed by measuring a small apparent cross section at energies below the threshold for ionization of the incident ions out of their ground states. Such a signal can be due to excited ions in the incident beam, but for Li-like ions such as C^{3+} and N^{4+} no long-lived excited states exist, since the $(1s2s2p)^4P$ levels are strongly autoionizing. Furthermore, in such cases threshold onsets will occur at the ionization potentials of the excited states, and none were found. Finally, the apparent cross section below threshold was usually negative in the present case and could be varied significantly by deliberate defocusing of the ion beam. Deliberate deflection of the ion beam was also observed to produce changes in the signal below threshold, but more dramatic changes could be produced by defocusing, without significant reduction in transmitted ion-beam current; thus the latter was used for diagnostic tests. Figure 4 shows the results obtained with an incident ion beam that was deliberately detuned to enhance the spurious cross section measured below threshold. The corrected cross section at 187 eV was obtained by directly subtracting the apparent cross section at 43 eV (below threshold) from the apparent cross section at 187 eV observed with the same ion-beam-tuning conditions. As shown in
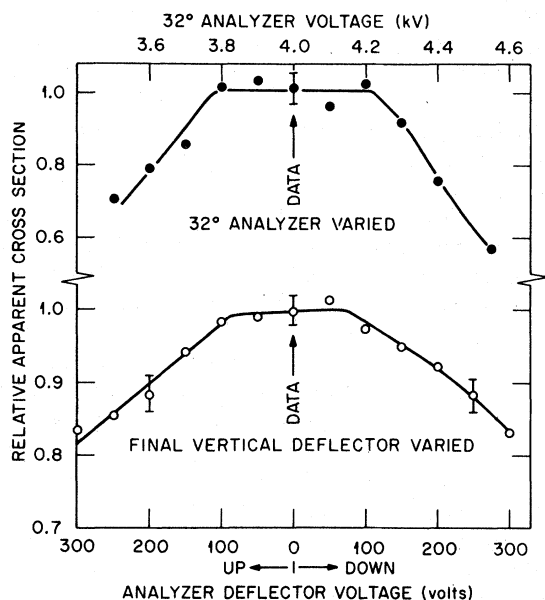

FIG. 3. Relative variation of apparent cross section for ionization of 29.5-keV C^{3+} by 187-eV electrons with changes in ion-beam optics. Lower curve is for change of voltage on the final vertical deflector, and upper curve is for change of voltage on 32° cylindrical analyzer. Arrows indicate selected operating points, and error bars are 1 standard deviation on counting statistics.
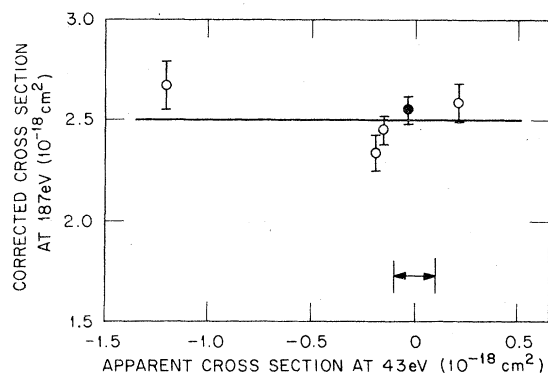
FIG. 4. Corrected cross section for ionization of C^{3+} by 187-eV electrons (deduced by subtracting the apparent cross section at 43 eV from the initially observed signal at 187 eV) plotted vs the spurious below-threshold value. Error bars are 1 standard deviation on counting statistics of both above- and below-threshold signals added in quadrature. The spurious signal could be "tuned" by ion-beam focusing, and bracketed arrows indicate the magnitude of this below-threshold signal allowed in normal data trials.

Fig. 4., the deduced "corrected cross section" is independent of the magnitude of the correction for a spurious, below-threshold signal up to an order of magnitude larger than tolerated in reported data. Essentially the problem could be eliminated in the present data by careful tuning of the ion beam, but more time was required for that endeavor than for actually accumulating data. Every data point was corrected by the subtraction of an apparent cross section acquired below threshold in conjunction with each set of measurements. The average absolute value of these independently applied corrections is 0.11×10^{-18} cm^2—less than 5% of the peak cross-section values.

As demonstrated, the correction applied to measured cross sections is reliable within a few percent from threshold to 187 eV, but this reliability may not extend to higher energies. The magnitude of the modulated portion of the photon background might be expected to increase with the electron beam space charge which does increase with energy. At a fixed energy the space charge increases linearly with electron current, and a test of measured ionization cross section versus electron current was performed with 280-eV electrons incident on C^{3+}. The electron current was varied from 1.3 to 3.0 mA, and the apparent ionization cross section was extrapolated linearly to zero electron current. This procedure produced a cross-section value about 3% lower than was measured under normal operating conditions (1.3 mA), with about ±2% s.d. statistical uncertainty. This test, together with results shown on Fig.

4, establishes that the measured cross sections are not strongly influenced by the level of background modulation encountered in the experiment. No additional correction was applied at higher energies where space charge modulation could be more severe, but for the background correction employed, an uncertainty of ±5% is chosen as appropriate to all of the data, since the measured correction at 280 eV did not depend strongly on electron current.

4. Ion-beam purity

Despite the purifier used to eliminate unwanted charge states in the incident beam, a small impurity was unavoidable in the C^{3+} case. The charge-to-mass ratios of C^{3+} and O^{4+} are identical to within 0.04%, and, once accelerated by the extraction at the ion source, the two species could not be separated. The purity of the C^{3+} beam relies on the elimination of oxygen in the source plasma. The content of O^{4+} in the beam can be analyzed by careful examination of currents passed by the purifier to the in-line Faraday cup as shown in Fig. 5. The C^{3+} and O^{4+} primary ions cannot be separated, but C^{2+} and O^{3+} formed by charge exchange along the flight path are easily separated by the purifier. The fractional content of O^{4+} in the incident beam can be estimated using the cross sections of Crandall et al.[36] for C^{3+} and O^{4+} charge exchange in H_2 as typical of charge exchange along the flight path. Since O^{5+} created by electron impact on the O^{4+} incident ions will not be passed by the post-collision analyzers to the channeltron, the presence of the incident O^{4+} requires only a small correction to the measured C^{3+} current. From measurements such as those illustrated in Fig. 5, performed on nine different occasions, the average correction to incident number of ions was (-1.30 ± 0.41)%.

The N^{4+} beam did not contain impurities.

5. Total uncertainties

Table II presents the uncertainties in measured cross sections arising from the difficulties discussed above. The relative uncertainty has been taken to be 2 standard deviations on counting statistics (about 90% confidence level). For each point the statistical uncertainty in counting at the energy of measurement was combined in quadrature with the statistics on the corresponding measurement of the below-threshold value. These below-threshold values were most often zero within counting statistics, but the statistical uncertainty in this determination was usually a little larger than the uncertainty at the energy where the cross section was being determined. Other
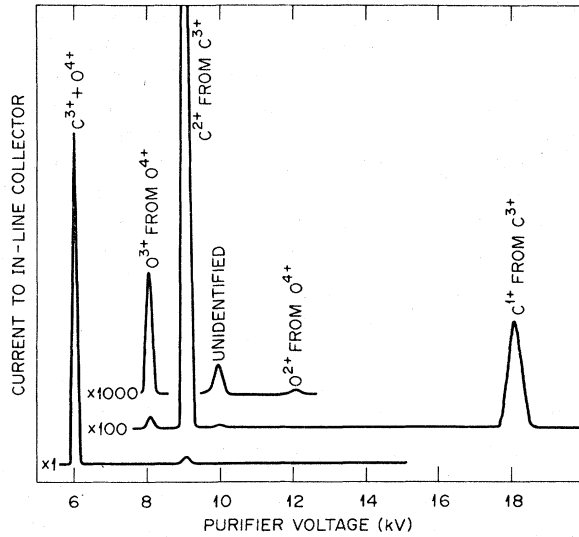
FIG. 5. Current passed to the in-line current collector as a function of charge purifier voltage. The peak at lowest voltage is the primary beam used for the experiment and remaining peaks are beam components formed by collisions in the beam transport from ion source to experiment. Comparisons of currents of C^{2+} (formed by C^{3+} electron capture) to O^{3+} (formed by O^{4+} electron capture) together with known cross sections for such electron capture (Ref. 36) allow determination of ratio of O^{4+} to C^{3+} in the primary beam.

sources of uncertainty could have small variation during a particular measurement or between measurements, but these contributions to the relative uncertainty should be smaller than counting statistics and were not quantitatively evaluated. A test on reproducibility was performed at 187 eV for C^{3+} data. At this energy there were 15 repeats of cross-section determination with deliberate variation of the tuning parameters and background levels. Thus, variation in this measurement

TABLE II. Uncertainties.

Source	Uncertainty in % C^{3+}	N^{4+}
Counting statistics (90% confidence level): typical value in % of peak cross section	±3.5	±10
Additional absolute uncertainty:		
Particle counting efficiency	±3	
Transmission to channeltron	±8	
Background modulation	±5	
Incident ion number	±2	
Incident electron number	±2	
Form factor evaluation	±3	
Quadrature sum:	±11.3%	±14.7%

could be larger than counting statistics since possible sources of systematic error were deliberately varied. The variation about the mean of the values at 187 eV was 3.4% (90% confidence level)—about the same as typical counting statistics on individual measurements.

The other uncertainties in Table II are the estimated absolute uncertainty which could be contributed by each of the sources listed. The systematic uncertainties are estimated at good confidence, intended to be equivalent to 90% confidence level on counting statistics. The quadrature sum of uncertainties is taken to be the total absolute uncertainty in the data.

III. RESULTS

A. C^{3+} ionization

Cross sections for electron-impact ionization of C^{3+} are presented in Fig. 6 and Table III. The relative uncertainty in each of the present data points is taken to be 2 standard deviations of counting statistics and is indicated by error bars. At 187 eV the total absolute uncertainty is indicated by the outer error bar. The measured value of Kunze,[21,37] shown on Fig. 6, is derived from plasma-observed rates and will be discussed later when rate coefficients are compared. The cross section determined by Donets[38,39] is obtained from observations of ions trapped in an electron-beam ion source (EBIS) and collided with a fixed-energy electron beam. This EBIS experiment is similar to the trapped-ion experiments of Hasted et al.[40,41] except that in the EBIS experiment the density of ions of a given charge evolves as a function of time in the presence of the intense, monoenergetic electron beam. In order to deduce individual ionization cross sections, a computer simulation of the time evolution of ion charge states (assuming only sequential single-electron ionization) is compared to the observed evolutions. Thus the EBIS results have significant uncertainties with difficulties similar to plasma rate measurements, but the ionizing electron source has more controlled and more specific energy and intensity than in plasma experiments.

A number of theoretical estimates are compared in Fig. 6. The recent results of Salop[42] employing a binary-encounter approach represents a completely classical calculation with all possible binary collisions (incident electron on any bound electron) simply summed to give the total cross section. The semiempirical estimate according to Lotz,[43] which is taken here as

$$\sigma(E) = 4.5 \times 10^{-14} \sum_j \frac{r_j}{I_j E} \ln \frac{E}{I_j} \text{ cm}^2, \qquad (4)$$
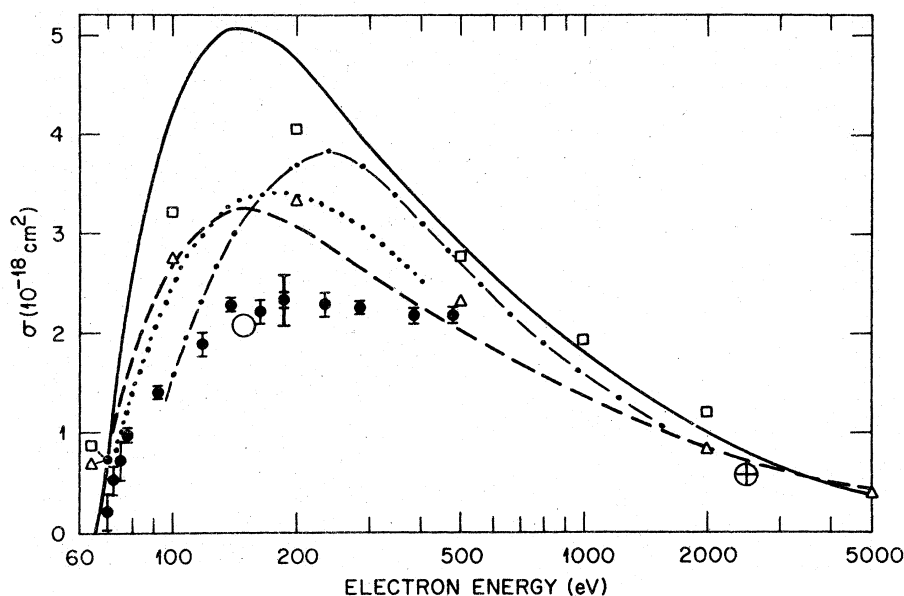
FIG. 6. Cross sections for electron-impact ionization of C^{3+} as a function of electron energy. Present data, ●; result inferred from rate measurement by Kunze (Ref. 21), ○; result of Donets (Ref. 38), ⊕; semiempirical estimate due to Lotz (Ref. 43), □; ECIP value by Barfield (Ref. 44), △; classical theory of Salop (Ref. 42), solid curve; Coulomb-Born calculation of Moores (Ref. 11), dotted curve; scaled Coulomb-Born value according to Golden and Sampson (Ref. 12), dashed curve; modified Bethe approximation of Hahn (Ref. 14), dot-dashed curve. Error bars are 2 standard deviations on counting statistics except heavy bar at 187 eV is absolute total uncertainty estimated at good confidence.

(where r_j is number of electrons in level j, I_j is the ionization energy of that level in eV, and E is the collision energy in eV), has been most widely used in plasma modeling, but in this case it

offers little improvement over the classical calculation.

The exchange classical impact parameter (ECIP) results shown on Fig. 6 were calculated by Bar-

TABLE III. Cross sections for ionization of C^{3+} and N^{4+}. Listed uncertainties are 2 standard deviations on counting statistics except for * where the value is the mean of 15 represented measurements with diagnostic variation of ion-beam parameters and the uncertainty is variation of the mean at 90% confidence level. Absolute uncertainty is obtained by combining these statistical uncertainties in quadrature with systematic uncertainty of ±10.7%.

C^{3+}		N^{4+}	
Electron energy (eV)	Cross section (10^{-18} cm^2)	Electron energy (eV)	Cross section (10^{-18} cm^2)
58	0	91	0
69	0.19 ± 0.08	103	0.20 ± 0.20
72.5	0.59 ± 0.14	112	0.34 ± 0.22
75	0.70 ± 0.20	120	0.56 ± 0.20
78	0.96 ± 0.07	136	0.82 ± 0.22
92	1.39 ± 0.06	140	0.86 ± 0.18
118	1.87 ± 0.11	161	1.17 ± 0.20
139	2.27 ± 0.07	190	1.20 ± 0.20
163	2.20 ± 0.14	236	1.42 ± 0.17
187	(2.33 ± 0.08)*	304	1.43 ± 0.16
235	2.28 ± 0.12	382	1.45 ± 0.14
286	2.25 ± 0.06	450	1.54 ± 0.16
386	2.17 ± 0.08	480	1.45 ± 0.16
481	2.18 ± 0.07	529	1.47 ± 0.14

field[44] after the development of Burgess.[45,46] This approach combines a symmetrized binary-encounter contribution (allowing for exchange) with a contribution obtained from a semiclassical integration over impact parameter. As pointed out by Barfield, the ECIP values can be changed by up to a factor of 2 depending on how the various contributing terms are represented. The cross sections calculated by Barfield are higher than present data by slightly more than the experimental uncertainty, but agree better than do the purely classical or semiempirical estimates. The recent distorted-wave-modified Bethe approximation by Hahn[14] gives cross sections between the ECIP and Lotz values at 300 eV and falls abruptly near threshold, so that it is lower than present data below 100 eV.

The best agreement between present data and theory is for the two calculations based on the Coulomb-Born approximation. The result calculated according to the prescription of Golden and Sampson[12] exploits the Coulomb-Born approximation for hydrogenic ions of infinite charge and applies a scaling procedure to obtain reasonable agreement with present data. Whether these scaled predictions will prove to be as reliable for ions of a different electron configuration, or even different charge, requires further experimental confirmation. The Coulomb-Born without exchange by Moores[11] is a direct calculation for C³⁺ and is very close to the ECIP and scaled Coulomb-Born. In previously published calculations using this theory for ions of lower charge, agreement with crossed-beams experiments has been better than ±25% for several cases. Thus the fact that the present data are 30% lower than this theory represents a minor discrepancy.

B. N⁴⁺ ionization

The cross sections for ionization of N⁴⁺ are presented in Fig. 7 and Table III. The cross section inferred from rate measurements[21] is discussed as a rate below, but is shown here to illustrate that agreement is not as good as in the C³⁺ case. The present data are somewhat closer to the classical theory and semiempirical (Lotz) estimate than were the C³⁺ data. Further data are needed to determine if there is a definite trend toward better agreement of these simplest theoretical estimates with increasing ionic charge. The modified Bethe approximation of Hahn[14] is well below present data near threshold, but rises quickly, crossing the measurements at 250 eV and peaking near the ECIP value at 500 eV. At the highest energies it approaches the scaled Coulomb-Born results.

The recent results of Donets and Ovsyannikov,[39] derived from study of the plasma of the EBIS ion source, give good agreement with present data for the lowest-energy data point they have measured (600 eV). However, the increase between this 600-eV value and their remaining higher-energy data is unexpected. Their value at 2.1 keV is about a factor of 2 higher than their previous EBIS-determined value.[38]

The agreement between present data for N⁴⁺ and the two Coulomb-Born based calculations[11,12] is excellent, except near 500 eV. In the present data for both C³⁺ and N⁴⁺ cases, the measured cross sections have not begun to decrease at the highest energy tested. At sufficiently high energy the cross sections must decrease with the correct quantum behavior, $\sigma \propto \log E/E$. However, none of the theories has included inner-shell excitation followed by autoionization, which can occur for both C³⁺ and N⁴⁺ $(1s2s^2)$ and $(1s2s2p)$ states. Golden and Sampson[47] estimate that this process would raise their cross sections by 20% at 400 eV for N⁴⁺, eliminating the apparent discrepancy with present data. Moores[11] concurs that this is the likely source of the discrepancy. Excitation of the $(1s2s^2)^2S$ state occurs near 420 eV for N⁴⁺ and near 300 eV for C³⁺. Excitation autoionization gives a large contribution to the total ionization cross sections for some singly charged ions,[24] and appears as a sudden enhancement in the cross section at the threshold for the excitation process. Extension of the present measurements to higher energies and a search for such excitation onsets are planned after modification to the apparatus.

It is noted that ionization of N⁴⁺ was previously attempted in a crossed-beams experiment by Bradbury, Sharp, Mass, and Varney,[48] but the experiment was not completed.

C. Rate coefficients

Rate coefficients have been determined from the present data. We obtained the values presented in Fig. 8 for C³⁺ and in Fig. 9 for N⁴⁺ by assuming a Maxwellian electron temperature and employing the computer code developed at the Joint Institute for Laboratory Astrophysics[49] to obtain rates from any known ionization or excitation cross sections. The rates determined are not very sensitive to the choice of cross-section value at high energies, and the binary-encounter results of Salop[42] were used to represent the cross section at energies above present data. Only ionization out of the ground state is included, but in some of the plasma experiments the densities are sufficiently high that appreciable population
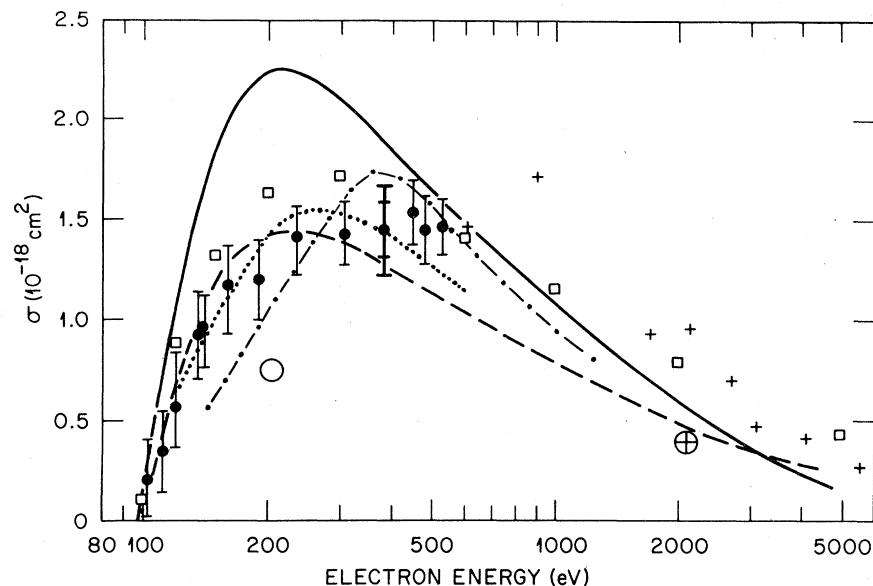
FIG. 7. Cross sections
for electron-impact ioni-
zation of N^{4+} as a function
of electron energy. Sym-
bols are the same as in
Fig. 6 with addition of re-
sults of Donets and Ov-
syannikov (Ref. 39), + .

of the $1s^22p(^2P)$ excited state could contribute to
observed ionization rates.

The uncertainty limits shown are just the un-
certainty in cross-section values with no allow-
ance for uncertainty in the conversion from cross
sections to rates. The rates presented are ex-
pected to be reliable at good confidence, within
the indicated uncertainty, although at the lowest
and highest temperatures the percentage of un-
certainty could be a little higher.

The measured rate of Kunze[21] and the ECIP-
predicted[15] rate for C^{3+} (Fig. 8) are in good agree-
ment with the present results. However, the
ECIP cross sections calculated by Barfield[44] and
shown on Fig. 6 would give a rate higher than
present data, while the ECIP rate shown on Fig. 8
gives a value slightly lower, illustrating the am-
biguity within ECIP. The classical theory rate
computed from Salop's cross sections[42] is shown
on Fig. 8 for comparison.
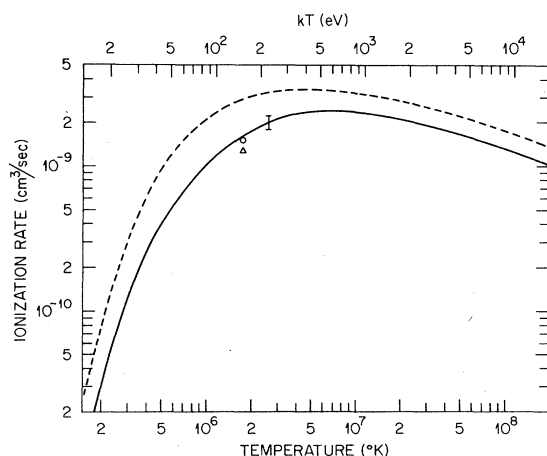
FIG. 8. Ionization rate for electron collision with C^{3+}
as a function of Maxwellian electron temperature. Pres-
ent result, solid curve; result from classical theory of
Salop (Ref. 42), dashed curve; ECIP calculated rate by
Burgess et al. (Ref. 15), △; measurement by Kunze
(Ref. 21), ○. Error bar is absolute uncertainty of cross-
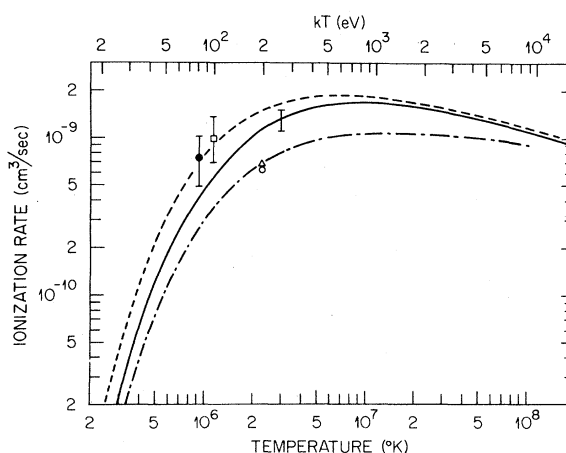section data.

FIG. 9. Ionization rate for electron collisions with N^{4+}
as a function of Maxwellian electron temperature.
Symbols are the same as Fig. 8 with addition of plasma-
observed rate measurements of Källne and Jones (Ref.
22), □; and of Rowan and Roberts (Ref. 23), ●; and the
ECIP calculated rate by Summers (Ref. 50), dot-dashed
curve.

For the N^{4+} case, however, discrepancies are significant (Fig. 9). Present results are a factor of 2 lower than the measurements of Källne and Jones[22] and of Rowan and Roberts[23] but are nearly a factor of 2 higher than the Kunze[21] measurement. The discrepancies are slightly larger than expected on the basis of estimated uncertainties in the plasma-observed results, but high plasma density in the Källne and Jones and the Rowan and Roberts measurements may influence the results. The ECIP-predicted rate[15,50] for N^{4+} is nearly the same as the Kunze measurement, so that the discrepancy between present results and ECIP calculated value is also significant.

The ECIP rate calculation by Summers[50] allows for excitation-deexcitation of excited states in the plasma. The Summers result plotted on Fig. 9 is for densities of 10^{12} cm^{-3} or lower where population of excited states is insignificant. At a density of 10^{16} cm^{-3} and a temperature of 10^6 K, Summers predicts an increase in the N^{4+} ionization rate of 45% due to $1s^2 2p(^2P)$ level population, while at 10^7 K the increase is only a few percent at most. The application of this percentage increase to the rate computed from present data would raise the value at 10^6 K from 4.7×10^{-10} cm^3/sec (plotted) to 6.8×10^{-10} cm^3/sec. Since the experiments of Rowan and Roberts[23] and Källne and Jones[22] were performed at densities near 10^{16} cm^{-3}, a comparison with present results should allow for ionization from excited states. When one makes the adjustment suggested by Summers' calculations, rates obtained from the present data are brought to within the uncertainties of these two plasma-observed rates.

*Present address: Center for Astrophysics, 60 Garden St., Cambridge, Mass. 02138.

[1]J. J. Thomson, Philos. Mag. 23, 449 (1912).

[2]O. Bely and H. Van Regemorter, Ann. Rev. Astron. Astrophys. 8, 329 (1970).

[3]G. H. Dunn, IEEE Trans. Nucl. Sci. NS23, 929 (1976).

[4]R. K. Peterkop, Sov. Phys. Dokl. 27, 987 (1963); R. K. Peterkop, Sov. Phys. JETP 16, 442 (1963).

[5]M. R. H. Rudge and M. J. Seaton, Proc. R. Soc. London Ser. A 283, 262 (1965).

[6]D. L. Moores, J. Phys. B 5, 286 (1972).

[7]D. L. Moores and H. Nussbaumer, J. Phys. B 3, 161 (1970).

[8]K. L. Aitken and M. F. A. Harrison, J. Phys. B 4, 1176 (1971).

[9]K. L. Aitken, M. F. A. Harrison, and R. D. Rundel, J. Phys. B 4, 1189 (1971).

[10]S. O. Martin, B. Peart, and K. T. Dolder, J. Phys. B 1, 537 (1968).

[11]D. L. Moores (private communication).

[12]L. B. Golden and D. H. Sampson, J. Phys. B 10, 2229 (1977).

[13]A. Burgess, D. G. Hummer, and J. A. Tully, Philos. Trans. R. Soc. A 266, 225 (1970).

[14]Y. Hahn, Phys. Rev. A 16, 1964 (1977).

[15]A. Burgess, H. P. Summers, D. M. Cochrane, R. W. P. McWhirter, Mon. Not. R. Astron. Soc. 179, 275 (1977).

[16]R. C. Isler, R. V. Neidigh, and R. D. Cowan, Phys. Lett. A 63, 295 (1977).

[17]A. L. Merts, R. D. Cowan, N. H. Magee, Jr., "The Calculated Output from a Thin Ion-Seeded Plasma," Report No. LA-6229 MS, Los Alamos Scientific Laboratory, Los Alamos, N.M. 85545 (1976).

[18]C. Breton, C. DeMichelis, and M. Mattioli, Nucl. Fusion 16, 891 (1976).

[19]R. V. Jensen, D. E. Post, W. H. Grasberger, C. B. Tarter, and W. A. Lokke, Nucl. Fusion 17, 1187 (1977).

[20]C. Jordan, Mon. Not. R. Astron. Soc. 142, 501 (1969); 148, 17 (1970).

[21]H.-J. Kunze, Phys. Rev. A 3, 937 (1971).

[22]E. Källne and L. A. Jones, J. Phys. B 10, 3637 (1977).

[23]W. L. Rowan and J. R. Roberts, National Bureau of Standards, Washington, D.C. 20234 (private communication).

[24]K. T. Dolder and B. Peart, Rep. Prog. Phys. 39, 693 (1976).

[25]M. F. A. Harrison, in Methods in Experimental Physics, Vol. 7A, edited by W. L. Fite and B. Bederson (Academic, New York, 1968), pp. 95-115.

[26]P. O. Taylor, Ph.D. thesis (University of Colorado, 1972) (unpublished) (Available through University Microfilms, Ann Arbor, Mich.)

[27]P. O. Taylor, D. Gregory, G. H. Dunn, R. A. Phaneuf, and D. H. Crandall, Phys. Rev. Lett. 39, 1256 (1977).

[28]D. C. Gregory, P. O. Taylor, G. H. Dunn, R. A. Phaneuf, and D. H. Crandall (unpublished).

[29]M. L. Mallory and D. H. Crandall, IEEE Trans. Nucl. Sci. NS23, 1069 (1976).

[30]G. A. Harrower, Rev. Sci. Instrum. 26, 850 (1955).

[31]P. O. Taylor, K. T. Dolder, W. E. Kauppila, and G. H. Dunn, Rev. Sci. Instrum. 45, 538 (1975).

[32]L. Harris and J. K. Beasley, J. Opt. Soc. Am. 42, 134 (1952).

[33]J. A. Ray and C. F. Barnett, IEEE Trans. Nucl. Sci. NS17, 44 (1970).

[34]D. H. Crandall, J. A. Ray, C. Cisneros, Rev. Sci. Instrum. 46, 562 (1975).

[35]R. A. Phaneuf, H. Kim, F. W. Meyer, and P. H. Stelson, Oak Ridge National Laboratory, Oak Ridge, Tenn. 37830 (private communication).

[36]D. H. Crandall, M. L. Mallory, and D. C. Kocher, Phys. Rev. A 15, 61 (1977).

[37]R. U. Datla, L. J. Nugent, H. R. Griem, Phys. Rev. A 14, 979 (1976).

[38]E. D. Donets, IEEE Trans. Nucl. Sci. NS23, 897 (1976).

[39]E. D. Donets and V. P. Ovsyannikov, Report No. P7-10780 of the Joint Institute of Nuclear Research, Dubna, USSR; translation ORNL-tr-4616 available from Technical Information Center, P. O. Box 62, Oak Ridge, Tenn. 37830.

[40]J. B. Hasted and G. L. Awad, J. Phys. B 5, 1719 (1972).

[41]M. Hamdam, K. Birkinshaw, and J. B. Hasted, J. Phys. B 11, 331 (1978).

[42]A. Salop, Phys. Rev. A 14, 2095 (1976).

[43]W. Lotz, Z. Phys. 216, 241 (1968).

[44]W. D. Barfield, IEEE Trans. Plasma Sci. PS-6, 71 (1978).

[45]A. Burgess, Proceedings of the Symposium on Atomic Collisions in Plasmas, Culham, England (UKAEA Rep. 4818), p. 63 (1964).

[46]A. Burgess and H. P. Summers, Mon. Not. R. Astron. Soc. 174, 345 (1976).

[47]L. B. Golden and D. H. Sampson (private communication).

[48]J. N. Bradbury, T. E. Sharp, B. Mass, and R. N. Varney, Nucl. Instrum. Methods 110, 75 (1973).

[49]D. H. Crandall, G. H. Dunn, A. Gallagher, D. G. Hummer, C. V. Kunasz, D. Leep, and P. O. Taylor, Astrophys. J. 191, 789 (1974).

[50]H. P. Summers, Mon. Not. R. Astron. Soc. 169, 663 (1974).